Drag-Free Satellite Control

Stephan Theil

Center of Applied Space Technology and Microgravity, University of Bremen,
Am Fallturm, 28359 Bremen, Germany

Summary. Scientific satellite missions trying to investigate questions regarding geodesy and fundamental physics have become increasingly dependent on ultra-low disturbance environments. The precision demanded by the experiments has risen continuously as experimenters strive to deepen their understanding. Standard attitude and orbital control systems are not capable of providing such an ultra-low disturbance environment which lead to the introduction of so-called *drag-free control systems*.

Drag-free control is an enabling technology with the capability to provide these ultra-low disturbance environments. The application of drag-free control systems is of course not limited to geodesy and fundamental physics. It is a useful technology for every mission that requires a low disturbance free-fall environment.

Drag-free control has come a long way since the introduction of the original drag-free concept by Benjamin Lange in 1964. The aim of this chapter is to give an introduction and overview about the drag-free technology and its implications for scientific satellite missions. In addition to the original drag-free concept and its advancements, the chapter introduces key technologies in sensors and actuators whose development was fueled by the application of the drag-free concept in scientific satellite missions. Moreover, problems and challenges connected to drag-free satellite control and the technologies involved are discussed, and current drag-free missions like LISA and its technology demonstrator LISA Pathfinder, MICROSCOPE, STEP, or GOCE are presented.

1 Introduction

1.1 The Drag-Free Satellite Principle

The motion of satellites on orbits around Earth is mainly determined by the gravitational field of the Earth. In addition to that, forces and torques are acting on the satellite which affect attitude and orbit. In 1964 B. Lange proposed to compensate these disturbing forces and torques using a control system to get a “force- and torque-free” satellite. Since the force due to interaction with

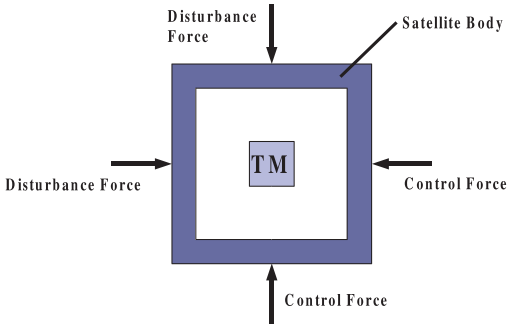

Fig. 1. Planar schematic of a drag-free satellite with its test mass (TM).

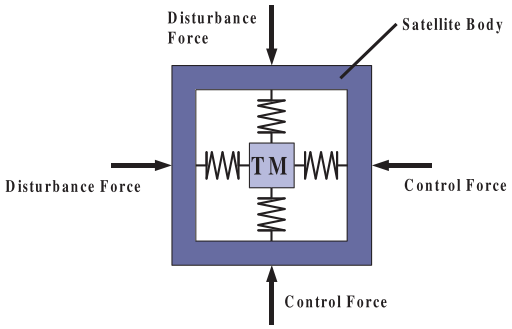

Fig. 2. Planar schematic of drag-free satellite with its test mass (TM) and coupling between satellite and test mass.

the upper atmosphere – which is denoted as air drag – is the main disturbance for satellites in low Earth orbits, the term "drag-free satellite" was introduced. The control system for compensation of the disturbance forces is called "drag-free control system."

The concept of a drag-free satellite involves centering a test mass inside a satellite. The test mass (or proof mass) is shielded by the surrounding satellite against the disturbances acting on the surface (see Fig. 1). As the test mass is free of external disturbances, it will follow a purely gravitational orbit.

To avoid a collision with the test mass, the satellite has to be controlled to follow the test mass. For that purpose the distance between satellite and test mass must be measured. This can be done by magnetic, electrostatic, or optical sensors. In all three cases the measurement cannot be obtained without applying a force on the test mass. Therefore a dynamic coupling exists between the satellite and the proof mass. This is denoted by the springs in Fig. 2. Due to this coupling the test mass inside the satellite is not free from external forces anymore. The coupling will perturb the orbit of the test mass. To minimize this effect the springs can be chosen to be very weak. But this has the disadvantage that the accuracy of the displacement measurement

between test mass and satellite may become poor. As an example consider the magnetic measurement which is more accurate if a stronger field is applied. So an optimum for the equivalent stiffness of the magnetic field can be found. The second way is to reduce the displacement of the satellite w.r.t. the test mass to put the test mass at the equilibrium point of the relaxed equivalent springs. This can only be achieved by precise control. It has the advantage that the residual acceleration on the whole satellite is minimized.

1.2 Review of Drag-Free Satellite Development

Similar systems to the drag-free system are known in microgravity research where airplanes were flown on a parabolic trajectory. This was done by keeping a small object centered in free space inside the cabin which is the basic principle of parabolic flights.

The first suggestions of the drag-free control concept for a satellite were made by several investigators independently. M. Schwarzschild (1961), R.A. Ferrell, G.E. Pugh (1959), G.J.F. MacDonald, C.W. Sherwin (1962), and B.O. Lange (1961) have proposed the drag-free satellite in various forms. Lange derived in his thesis [8] the nine-degree-of-freedom equations of motion. He evaluated and discussed special cases of the equations of motions and gave a comprehensive list of applications for the drag-free satellite. In 1970, J.D. Powell developed the first analog estimator for estimating the center of mass of a spinning drag-free satellite in two-dimensional space.

The first successfully flown drag-free satellite was TRIAD I [3]. The disturbance compensation system DISCOS was developed at Stanford University under responsibility of D.B. DeBra. The drag-free control system compensated the disturbances on the satellite in three degrees of freedom. It reached a residual acceleration on the satellite of about $5 \cdot 10^{-11}\,\mathrm{m\,s^{-2}}$ when averaged over 3 days. The second drag-free satellite application was the TIP II satellite which was partially drag-free in one axis [11]. This first generation of drag-free satellites was designed to improve the ephemeris prediction of the U.S. Navy's navigation satellite system TRANSIT.

The next generation of drag-free satellites is used for scientific missions like the Gravity Field and Steady-State Ocean Circulation Explorer (GOCE) mission, Gravity Probe B (GP-B), the Satellite Test of the Equivalence Principle (STEP), and the Laser Interferometer Space Antenna (LISA) mission. The difference with respect to the first generation is, on one hand, that in some missions more than one test mass is used which can improve the overall performance of the drag-free control system; on the other hand, the quality of the "zero-g" environment is orders of magnitudes better than for the first generation. Especially this improvement made drag-free control to one of the enabling technologies for current and future fundamental physics space missions.

2 Dynamic Model

To design a control system for the dynamics of a drag-free satellite, the equations of motion are needed. This chapter will show the significant differences to conventional satellites.

2.1 Equations of Motion

Satellite Equations of Motion

The equations of motion for the satellite are similar to the dynamics of conventional satellites. One term is added to the equation for the translational motion as well as to the equation for the rotational motion. They become

$$\ddot{\boldsymbol{r}}^i_{i,b} = \boldsymbol{g}^i_{i,b}\left(\boldsymbol{r}^i_{i,b}\right) + \boldsymbol{f}^i_{\text{control}} + \boldsymbol{f}^i_{\text{dist}} + \boldsymbol{f}^i_{\text{coupl,sat}} \tag{1}$$

where $\ddot{\boldsymbol{r}}^i_{i,b}$ is the acceleration of the satellite relative to the inertial frame expressed in the inertial frame; $\boldsymbol{g}^i_{i,b}$ the gravitational acceleration as a function of the satellite's position; $\boldsymbol{f}^i_{\text{control}}$ the specific control force; $\boldsymbol{f}^i_{\text{dist}}$ the sum of all disturbance-specific forces acting on the satellite; and $\boldsymbol{f}^i_{\text{coupl,sat}}$ the specific force on the satellite due to the coupling between satellite and all test masses, and sum of coupling forces from each single test mass.
And

$$\dot{\boldsymbol{\omega}}^b_{i,b} = \left(\mathcal{I}^b_b\right)^{-1}\left[\boldsymbol{T}^b_{\text{control}} + \boldsymbol{T}^b_{\text{dist}} + \boldsymbol{T}^b_{\text{coupl,sat}} - \boldsymbol{\omega}^b_{i,b} \times \left(\mathcal{I}_b \boldsymbol{\omega}^b_{i,b}\right)\right] \tag{2}$$

$$\dot{\mathbf{q}}^b_i = \frac{1}{2}\,\hat{\boldsymbol{\omega}}^b_{i,b} \odot \mathbf{q}^b_i \tag{3}$$

where $\boldsymbol{\omega}^b_{i,b}$ is the angular velocity of the satellite w.r.t. inertial frame expressed in body-fixed coordinate frame; $\mathcal{I}^b_b$ the moments of inertia tensor of the satellite; $\boldsymbol{T}^b_{\text{control}}$ the control torques applied for attitude control expressed in the body-fixed frame; $\boldsymbol{T}^b_{\text{dist}}$ the disturbance torques acting on the satellite expressed in the body-fixed frame; $\boldsymbol{T}^b_{\text{coupl,sat}}$ the torques generated from satellite–test mass coupling expressed in the body-fixed frame, and sum of coupling torques generated by each single test mass; and $\mathbf{q}^b_i$ the attitude quaternion describing the orientation of the satellite body-fixed frame w.r.t. the inertial frame.

The term $\hat{\boldsymbol{\omega}}^b_{i,b}$ is the quaternion representation of the angular velocity. The operator $\odot$ is the quaternion multiplication.

Test Mass Equations of Motion

The equations of motion of a test mass relative to the satellite can be derived from the equations of motion in the inertial frame. This relative motion of the test mass is conveniently expressed in the rotating sensor frame which is

fixed to the satellite body. For that reasons terms due to the rotation and acceleration of the satellite will be included in the equation of motion for the test mass. Then the translational motion of the test mass w.r.t. the satellite-fixed sensor frame can be described as

$$\begin{aligned}\ddot{\boldsymbol{r}}^b_{b,tm} =& \Delta\boldsymbol{g}^b_{b,tm} - \boldsymbol{f}^b_{\text{control}} - \boldsymbol{f}^b_{\text{dist}} - \boldsymbol{f}^b_{\text{coupl,sat}} + \boldsymbol{f}^b_{\text{coupl,tm}} \\ & - 2\,\boldsymbol{\omega}^b_{i,b} \times \dot{\boldsymbol{r}}^b_{b,tm} - \dot{\boldsymbol{\omega}}^b_{i,b} \times \boldsymbol{r}^b_{b,tm} - \boldsymbol{\omega}^b_{i,b} \times \left(\boldsymbol{\omega}^b_{i,b} \times \boldsymbol{r}^b_{b,tm}\right) ,\end{aligned} \tag{4}$$

where $\boldsymbol{r}^b_{b,tm}$ is the position of the test mass relative to the satellite body frame; $\boldsymbol{g}^b_{b,tm}$ the gravitational acceleration as a function of the test mass position; $\boldsymbol{f}^b_{\text{coupl,tm}}$ the specific force acting on the test mass due to satellite–test mass coupling; and $\boldsymbol{\omega}^b_{i,b}$ the rotation of the satellite w.r.t. the inertial frame.

The formulation of the equations of motion for the test mass attitude w.r.t. the sensor is based on the conservation of the angular momentum. The test mass inside the satellite is shielded from all external nongravitational forces and torques. So the equation for the rotational motion can be written as

$$\begin{aligned}\dot{\boldsymbol{\omega}}^{tm}_{b,tm} = & \left(\mathcal{I}^{tm}_{tm}\right)^{-1} \left[\boldsymbol{T}^{tm}_{coup,tm} + \boldsymbol{T}^{tm}_{\text{gg,tm}} - \left(\boldsymbol{\omega}^{tm}_{i,b} + \boldsymbol{\omega}^{tm}_{b,tm}\right) \left(\mathcal{I}^{tm}_{tm} \left(\boldsymbol{\omega}^{tm}_{i,b} + \boldsymbol{\omega}^{tm}_{b,tm}\right)\right)\right] \\ & - \dot{\boldsymbol{\omega}}^{tm}_{i,b} ,\end{aligned} \tag{5}$$

where $\boldsymbol{\omega}^{tm}_{b,tm}$ is the angular velocity of the test mass relative to the satellite body-fixed frame expressed in the test mass body-fixed frame; $\mathcal{I}^{tm}_{tm}$ the moments of inertia matrix of the test mass; $\boldsymbol{T}^{tm}_{\text{gg,tm}}$ the gravity-gradient torque for the test mass from Earth gravity field as well as from gravity gradient inside the satellite; and $\boldsymbol{T}^{tm}_{coup,tm}$ the torque on the test mass due to satellite–test mass coupling.

The attitude of the test mass w.r.t. the sensor frame can be expressed by quaternions. The differential equation describing the kinematics of the test mass w.r.t. the satellite is written as

$$\dot{\mathbf{q}}^{tm}_b = \frac{1}{2}\,\hat{\boldsymbol{\omega}}^{tm}_{b,tm} \odot \mathbf{q}^{tm}_b \,. \tag{6}$$

2.2 Forces and Torques

To model the dynamic behavior of satellite and test masses, the forces and torques acting on both have to be modeled too. There exist forces and torques acting on both – satellite and test masses – as well as forces and torques acting on the satellite only.

The first group includes the effect of gravitation between celestial body, satellite, and test masses as well as interaction of satellite and test masses via the coupling which is inherent in a measurement and/or positioning system for the test masses.

Forces and torques acting on the satellite only are:

- Controlled actuation forces and torques for satellite attitude and translation control (ATC)
- Forces and torques due to interaction with the upper atmosphere (for low Earth orbits)
- Electromagnetic radiation-induced forces and torques on the satellite surface
- Torques due to interaction of satellite components with the external magnetic field
- Force and torque impulses from space debris and meteoroid hits

The following subsections will focus on the forces acting directly on the test masses. These forces are due to the coupling between satellite and test masses as to due to gravitational attraction.

Test Mass–Satellite Coupling

If the drag-free satellite houses only one test mass, the equations of motion become relatively simple as denoted in Sect. 2.1. If more than one test mass is onboard the satellite the dynamics of all bodies (satellite and test masses) are connected via the coupling force and gravitational attraction.

We assume that the satellite is connected to a test mass via a sensor system which produces a force and a torque on the satellite. This force and torque can be described as a function of the test mass states w.r.t. the body-fixed frame. For the force and torque on the satellite produced by the coupling to test mass j, we can write:

$$\begin{aligned} \boldsymbol{F}_{sat,j} &= \boldsymbol{f}_{\mathrm{F},sat,j}\left(t, \boldsymbol{r}^b_{b,j}, \dot{\boldsymbol{r}}^b_{b,j}\right) \\ \boldsymbol{T}_{sat,j} &= \boldsymbol{r}^b_j \times \boldsymbol{f}_{\mathrm{F}}\left(t, \boldsymbol{r}^b_{b,j}, \dot{\boldsymbol{r}}^b_{b,j}\right) + \boldsymbol{f}_{\mathrm{T},sat,j}\left(t, \mathbf{q}^j_b, \boldsymbol{\omega}^j_{b,j}\right) \end{aligned} \tag{7}$$

The forces and torques for all test masses j have to be added. They render the total force and torque due to coupling which are part of the equations of motion (see (1),[1] (2), and (4)).

The force and the torque on the test mass due to the coupling with the satellite is the same but in the opposite direction. In addition the test mass might experience forces and torques from a coupling with other test masses. In case there is a coupling to a second test mass k, the force and torque become:

$$\begin{aligned} \boldsymbol{F}_j =& \boldsymbol{f}_{\mathrm{F},sat,j}\left(t, \boldsymbol{r}^b_{b,j}, \dot{\boldsymbol{r}}^b_{b,j}\right) + \boldsymbol{f}_{\mathrm{F},j,k}\left(t, \boldsymbol{r}^b_{b,j}, \dot{\boldsymbol{r}}^b_{b,j}, \boldsymbol{r}^b_{b,k}, \dot{\boldsymbol{r}}^b_{b,k}\right) \\ \boldsymbol{T}_j =& \boldsymbol{f}_{\mathrm{T},sat,j}\left(t, \mathbf{q}^j_b, \boldsymbol{\omega}^j_{b,j}\right) + \boldsymbol{f}_{\mathrm{T},j,k}\left(t, \mathbf{q}^j_b, \boldsymbol{\omega}^j_{b,j}, \mathbf{q}^k_b, \boldsymbol{\omega}^k_{b,k}\right) \end{aligned} \tag{8}$$

[1] The specific force in (1) is the force divided by the mass of the satellite, respectively, test mass.

The functions f for the coupling force and torque can be depending on the sensor type nonlinear in the states. In a first approximation a linear coupling (spring-damper system) is used.

Gravitational Attraction Between Satellite and Test Masses

For most satellite applications the gravitational field created by the satellite is usually negligible. In case of the drag-free satellite, it becomes a force which connects the dynamics of satellite and test masses. This force can be reduced or compensated by design, e.g., placing the test mass in the center of mass of the satellite. Since this configuration is not always possible – e.g., if more than one test mass is used – the gravitational force between satellite and test mass has to be taken into account.

If the structure of the satellite is stiff and has no moving parts, the gravitational attraction between satellite and test mass is constant. However, if there is a transient deformation, e.g., due to thermal expansion or sloshing of liquid (fuel), there are moving masses which make the gravitational attraction force between satellite and test mass a time-varying quantity (see [14]).

Gravity-Gradient Acceleration

In the equation of translational motion for the test mass 4, the term $\Delta \boldsymbol{g}_{b,tm}$ denotes the gravity-gradient acceleration of the test mass. It is the difference in the gravitational acceleration of satellite and test mass

$$\Delta \boldsymbol{g}_{b,tm} = \boldsymbol{g}_{tm} - \boldsymbol{g}_{b}. \tag{9}$$

If we neglect the gravitational attraction between satellite and test mass, the gravitational acceleration on each body can be treated independently. In contradiction to conventional satellites, the gravitational force on the satellite cannot be assumed to be independent from the attitude of the satellite. Since the center of gravity might move with the attitude of the satellite, the gravitational force resp. acceleration changes with the attitude. Though this is a very small effect it should be considered in the modeling of a drag-free satellite (see [7]).

3 Technology

The increasing interest by the scientific community in the drag-free idea and its applications has fueled the technological development in this area. In recent years a number of different concepts for sensors and actuators has been proposed and developed. This section will give a brief overview about the different technologies that are out there.

3.1 Sensors

A central part of the drag-free control system is of course the drag-free sensor. Most of the sensors available today are custom made for specific applications. Nevertheless three main categories can be identified that can be used to classify the different sensors: namely, the mode of operation the sensor is used in, the measurement principle, and the discharging mechanism.

Mode of Operation

The mode of operation is the main category used to classify different sensors as it is directly connected to the application of the sensor. In general one can distinguish between two different modes of operation, the so-called accelerometer mode (AM) and the displacement mode (DM).

The DM concept uses a free-floating test mass. The displacement of this test mass relative to its housing is measured by the sensor and this signal is used to control the satellite to follow the test mass to drive the relative displacement to zero, thus minimizing the external disturbances on the test mass. The test mass will therefore follow a purely gravitational orbit. The DM concept is used most often in satellites where the drag-free sensor is the experiment itself, because of the very high sensitivity of the sensor in this mode. However the DM concept has the drawback that it requires complicated discharging mechanisms since a permanent grounding of the test mass via a gold wire is not possible. An example for a sensor that is used in displacement mode is the LISA Pathfinder sensor (see Fig. 3).

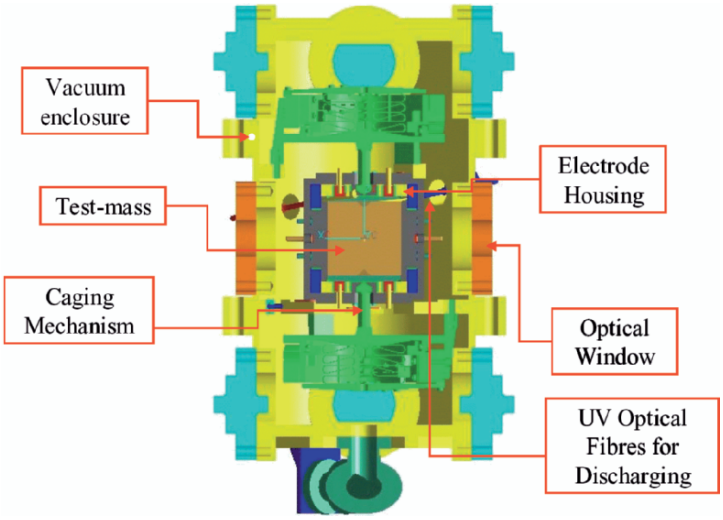

Fig. 3. LISA Pathfinder sensor.

The AM concept, on the other hand, uses the relative displacement measurements of the test mass w.r.t. the housing in an internal suspension control loop. This loop drives the displacement to zero by forcing the test mass to follow the satellite. The force that is needed to drive the displacement to zero is a measure for the acceleration on the satellite. This is the reason why the AM concept is most often used in missions that require highly sensitive accelerometers. The measurements of theses accelerometers are then fed back to the drag-free control system that uses the acceleration measurements to minimize the disturbances on the satellite thus providing a low disturbance environment for experiments onboard the spacecraft. Although less accurate the AM concept has the big advantage that permanent grounding of the test mass via a gold wire is possible.

Measurement Principle

The two most commonly used measurement principles that are used in drag-free sensors today are the electrostatic measurement principle and magnetic measurement principle.

Electrostatic Measurement Principle

In the electrostatic measurement principle, the relative displacement between the test mass and its housing is measured through a series of electrodes that are distributed around the test mass. An electrode and the opposing test mass area are forming a condenser. These condensers act as capacitive detectors. Two different methods have been proposed to measure relative displacement and attitude based on this setup, namely the gap-sensing and the slide-sensing method. Concerning the gap-sensing method, as the test mass moves relative to its housing the gap between the test mass and the electrode varies. This leads to a variation in the electric field which can be measured. Therefore the capacitive difference between the electrode and the test mass is a measure for the displacement of the test mass w.r.t. the electrode and thus the housing. If the slide-sensing method is applied, the test mass slides over the electrodes. The gap between the electrode and the test mass is constant but the overlapping area varies. The strength of the electric field depends on this overlapping area.

Magnetic Measurement Principle

A very interesting application of magnetic measurement principles is the superconducting quantum interference device (SQUID) that is used in the STEP sensor (see Fig. 4). SQUIDs combine a measurement sensitivity of as little as 10^{-15} m with the stability possible in a 2 K cryogenic environment using supercurrents.

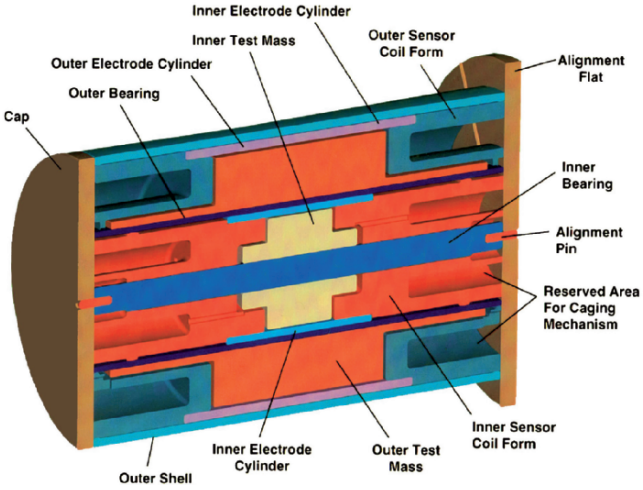

Fig. 4. STEP sensor.

Discharging Mechanism

The two most commonly used discharging methods include the ultraviolet-lamp (UV-lamp) and the gold wire. Which type of discharging mechanism has to be used is heavily influenced by the mode of operation that is used for the sensor. The most simple discharging method is the gold wire. Here the test mass is permanently grounded through the connection of the test mass with the housing via the gold wire. However the gold wire does limit the sensitivity of the sensor and cannot be used at all in case the test mass has to be free floating as in the displacement mode. This means that whenever the sensor shall be used in DM other means of discharging have to be applied. Unlike the gold wire the UV-lamp can be applied even if the test mass is free floating. The lamp emits ultraviolet photons which are used to release photoelectrons from the surface of the test mass. The freed electrons are then redistributed to neutralize the charge of the test mass. The UV-lamp does not limit the sensitivity of the sensor in the way the gold wire will but it is a very complex device that requires the charge on the test mass to be measured.

3.2 Actuators

As drag-free control systems are used to provide ultra-low disturbance environments, they usually require very low thrust levels. These low thrust demands combined with a demand for very small and accurate thrust steps gave rise to the development of new micropropulsion systems. These micropropulsion systems usually generate proportional thrust commands and operate in the thrust range from 0.1 to 100 μN. Different concepts and principles have

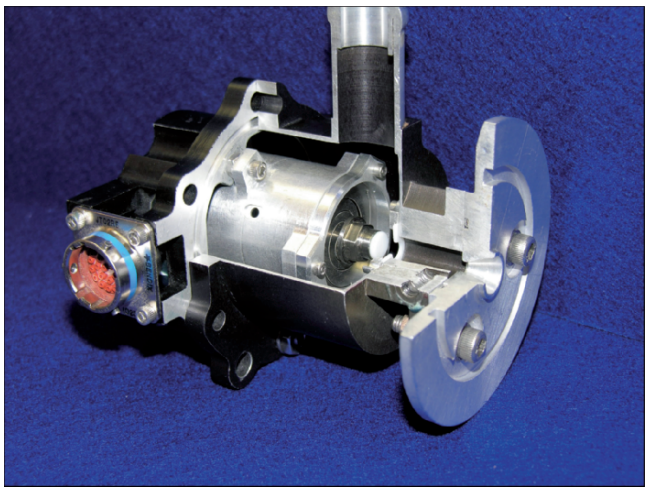

Fig. 5. Helium proportional thruster.

been proposed. The four most commonly used micropropulsion systems will be introduced in this section.

Helium Proportional Thrusters

The concept for Helium proportional thrusters has been developed for the Gravity Probe B mission and builds a synergy between the propulsion system and the temperature control of the cryogenic dewar. To stabilize the temperature inside the dewar, Helium is constantly vented. Instead of just venting the Helium the idea came up to use this Helium to produce the thrust for the control system. The Helium proportional thrusters produce a continuously variable thrust which is controlled by an internal control loop (Fig. 5).

Micropropulsion Cold Gas Thrusters

Micropropulsion cold gas systems are very similar to standard cold gas systems that are able to provide proportional thrust. They differ mainly in the thrust range. A very recent concept has been proposed by the Ångström Space Technology Centre at the University of Uppsala in Sweden. They have used microelectromechanical systems (MEMS) techniques to develop an all-in-one thruster that includes everything from propellant reservoir to control electronics (Fig. 6).

Field Emission Electric Propulsion

Field emission electric propulsion (FEEP) thrusters are ion thrusters that extract ions from a reservoir of liquid metal. The ions are accelerated in a strong electric field. Similar to the other propulsion concepts the FEEP thrusters are

Fig. 6. Micropropulsion cold gas thruster.

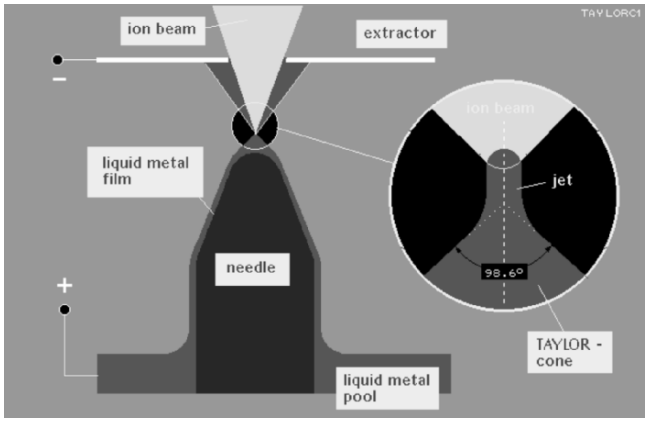

Fig. 7. FEEP concept (needle emitter).

able to produce a proportional thrust in the μN range. FEEP thrusters are capable of delivering very low thrust with very high accuracy and controllability. In addition fuel consumption is very low (Fig. 7).

Colloid Thrusters

The principle of the colloid thrusters is very similar to the FEEP concept. Colloid thrusters work by electrostatically accelerating a spray of charged, submicron diameter droplets of a conducting, nonmetallic liquid. They have a very small specific impulse and very low noise levels.

4 Missions

For the drag-free satellite several applications exist. First it can be used for geodesy. The higher harmonics of the Earth's gravitational potential perturb the orbit of a satellite. By observing the flight path of the satellite, the higher harmonics of the gravitational field can be determined. Another way for determining the gravitational potential is the measurement of the gravity gradient. The ESA mission GOCE (gravity field and steady-state ocean circulation explorer mission) has a payload consisting of two accelerometers each having a test mass which are measuring the gradient of the gravity field. The satellite is flown drag-free to reduce the disturbances and to reduce the dynamical range of the accelerometers [15].

A second application of drag-free satellites is aeronomy. Conventionally the density of the upper atmosphere is determined by observing the change in the period of a satellite's orbit. This depends on the averaging over one or more orbits. Instantaneous measurements at high frequency cannot be obtained using this method. The test mass onboard the satellite provides a signal for the drag-free control system. In operation, the control system can be used to measure instantaneously the force from the upper atmosphere as well as other forces (e.g., from radiation pressure). So every drag-free mission can obtain data for aeronomy (see [4]).

A further and most recent application is the utilization of drag-free satellites to provide a "real" zero-g or free-fall environment. This is used in a number of current and planned future missions. Especially experiments on fundamental physics are demanding a very low level of disturbances. The following missions will utilize a drag-free control system:

1. *Gravity Probe B (GP-B).* Test of relativistic effects on a gyroscope: the geodetic effect and the frame-dragging (or Lense–Thirring) effect
2. *Satellite Test of the Equivalence Principle (STEP).* Test of the weak equivalence principle
3. *MICROSCOPE.* Test of the weak equivalence principle at a lower level (precursor mission to STEP)
4. *Laser Interferometer Space Antenna (LISA).* Detection of gravitational waves
5. *HYPER.* Spatial mapping of the Lense–Thirring effect using atomic interferometers

All of them are going beyond the initial idea of one test mass shielded by the satellite. So in case of STEP, eight test masses are arranged in four differential accelerometers. Onboard the LISA spacecraft the baseline design uses two test masses. In addition to that the attitude of the test masses w.r.t. the LISA satellite is important for this experiment because the test masses are acting as mirrors for the laser beams between the satellites of the LISA constellation. It can be seen that the drag-free technology is becoming more

and more important for scientific satellite missions which need a very low disturbance environment.

In the following sections, a few of the missions named above are described with a focus on the drag-free control system.

4.1 Gravity Probe B

Gravity Probe B is the relativity gyroscope experiment developed by NASA and Stanford University to test two extraordinary, unverified predictions of Albert Einstein's general theory of relativity.

The experiment will measure, very precisely, tiny changes in the direction of spin of four gyroscopes contained in an Earth satellite orbiting at 640 km altitude directly over the poles. The quality of the disturbance environment provided by the Gravity Probe B spacecraft will enable the gyroscopes to provide an almost perfect space–time reference system. They will measure how space and time are warped by the presence of the Earth, and, more profoundly, how the Earth's rotation drags space–time around with it. These effects, though small for the Earth, have far-reaching implications for the nature of matter and the structure of the Universe.

The GP-B satellite was launched on 20 April 2004 from Vandenberg Air Force Base, CA, USA. After the in-orbit checkout phase, it will start its experimental measurement phase where the ATC system maintains the residual acceleration on the satellite below a level of $10^{-12} \times g$. The ATC (= drag-free control system) uses the suspended gyroscopes (spherical test mass) as the drag-free sensor. This measurement is obtained using the magnetic measurement principle based on a SQUID. To get the superconductivity for the SQUID and to reduce thermal noise, the experiment is contained in a liquid helium filled dewar. The boil-off gas from the dewar is used for ATC of the spacecraft. The Helium proportional thrusters which were especially developed for Gravity Probe B are used as the actuators to provide a six degrees of freedom control.

4.2 LISA and LISA Pathfinder

The LISA is a joint mission with NASA. It is a three-spacecraft mission, designed to detect the gravitational waves in space given out when very massive objects undergo strong acceleration. LISA will be the first mission to try and detect them from space. To achieve that goal, the relative position of several solid blocks placed in different spacecraft, 5 million kilometers apart, will have to be constantly monitored with high accuracy using laser-based techniques. A gravitational wave passing through the spacecraft will change the separations between them, thereby revealing itself. The existence of gravitational waves follows from Einstein's theory of general relativity. When a massive body is accelerated, or its motion is disturbed, it should "radiate."

This radiation takes the form of gravitational waves, a kind of feeble emission that should affect any type of matter. In particular, a solid body should vibrate if a gravitational wave hits it. No technique yet exists to detect the resulting vibrations. However, using laser interferometry, it is possible to monitor how the distance between solid bodies varies when a gravitational wave passes by.

Each of the three LISA spacecraft will carry two telescopes with associated lasers and optical systems. Pointing in directions separated by 60°, the telescopes in each spacecraft will communicate with the other two spacecraft, located at the other two corners of an equal-sided triangle. Apart from the complexity of aiming the laser beams from one small spacecraft to another across 5 million kilometers of space, LISA has to deal with other forces besides gravitational waves which will alter the separation of the spacecraft, e.g., the solar pressure.

The spacecraft must sense the extraneous forces and counteract them. The central part of each optical system will be a cube with a side length of 4 cm, made from a gold–platinum alloy. This test mass will float freely in most of its degrees of freedom. Acting as a reflector for the laser beams, the cube will provide the benchmark for measuring the distance between spacecraft.

The forces and torques acting on the satellite have to be canceled out by the drag-free control system. The position and attitude of the two test masses onboard each spacecraft are measured using an electrostatic measurement principle. The same principle is used to suspend the masses fully or in selected degrees of freedom. The thruster system is planned to be made up of FEEP thrusters. They will provide tiny control forces and torques which are needed to control the spacecraft in the required accuracy. The residual acceleration on the test masses shall be below $10^{-16}\,\mathrm{m\,s^{-2}}$ in the bandwidth between 10^{-4} and 10^{-1} Hz [5, 6, 12].

Currently ESA and NASA are developing and building the technology demonstrator LISA Pathfinder. Launch is scheduled in 2008. LISA Pathfinder shall demonstrate and test new technologies developed for LISA. The drag-free control system including sensors and actuators is among these new technologies to be tested.

4.3 STEP

The STEP is a joint European–U.S. space project to investigate one of the most fundamental principles in physics, the equivalence of inertial and passive gravitational mass. STEP will advance the sensitivity of the equivalence principle tests by six orders of magnitude, into regions where the principle may break down. A violation of equivalence at any level would have significant consequences for modern gravitational theory.

The STEP experiment is conceptually a modern version of Galileo Galilei's free-fall experiment, in which he is said to have dropped two weights from the

Leaning Tower of Pisa to demonstrate that they fall at the same rate. Any difference in the ratio of inertial to passive gravitational mass of the weights results in a difference in the rate of fall. In STEP, the masses are in free fall in an orbit around the Earth and if there is a violation of the equivalence principle they tend to follow slightly different orbits.

The STEP satellite will carry four of these differential accelerometers to test a range of different materials and of course for redundancy. The spacecraft will have a nearly circular orbit at an altitude of about 550 km. For thermal stability eclipses have to be avoided. Therefore a Sun-synchronous dusk-dawn orbit is chosen which will prevent the spacecraft from passing through the Earth's shadow during its 6-month lifetime.

Due to the low altitude of STEP's orbit, the interaction with the Earth's atmosphere is the main disturbance for the experiment. Unfortunately it occurs at the same frequency as the science signal. This disturbance has to be reduced to a level of $10^{-14}\,\mathrm{m\,s^{-2}}$ in the bandwidth of $10^{-6}\,\mathrm{Hz}$ around the measurement signal [13].

STEP is mainly developed at the W.W. Hansen Experimental Physics Laboratory of Stanford University. It inherits a lot of technologies from the recently launched Gravity Probe B mission. For example the test mass position is measured applying the magnetic measurement principle using SQUIDs. The experiment is also carried out in a cryogenically cooled environment to reduce the thermal noise and to enable the superconductivity needed for the magnetic suspension and the SQUIDs. The boil-off from the Helium is again used for the microthrust propulsion needed for the drag-free control system.

4.4 GOCE

The GOCE is dedicated to measuring the Earth's gravity field and modeling the geoid with extremely high accuracy and spatial resolution. It is scheduled for launch in 2006.

From its mission objective, GOCE does not need to have a free-fall environment. Nevertheless it carries a very sensitive gradiometer onboard which is sensitive to the very small gravity gradient along the spacecraft. To allow the measurement of this tiny gradient, the disturbances have to be reduced below the level of $2.5 \cdot 10^{-8}\,\mathrm{m\,s^{-2}\,Hz^{-1/2}}$ in the measurement bandwidth between 5 and 100 mHz [1, 2]. For that reason a drag-free control system is applied to cancel out the disturbances.

This control system has a second effect on the orbit of the satellite. Since it is now following a purely gravitational orbit there is no orbit decay due to the interaction with the upper atmosphere. This allows to have the GOCE satellite in a very low orbit (250 km) for a mission time of 2 years.

4.5 MICROSCOPE

MICROSCOPE (Microsatellite a trainée Compensée pour l'Observation du Principe d'Equivalence) is a CNES/ESA collaborative mission to test the

equivalence principle (EP) in space to a precision of one part in 10^{15} (10^{18} for STEP, see Sect. 4.3). Even with the simplest experiment in space, the precision of the test can be improved by 2–3 orders of magnitude over the best ground-based and lunar laser-ranging tests.

The MICROSCOPE payload comprises two differential electrostatic accelerometers, one testing a pair of materials of equal composition (platinum–platinum), to provide an upper limit for systematic errors, the other testing a pair of materials of different composition (platinum–titanium) as the EP test proper. As on STEP, the test masses in the MICROSCOPE payload are concentric hollow cylinders. Unlike STEP, the problem of test mass charging is eliminated by a thin gold grounding wire.

To separate the signal frequency from error sources, the spacecraft will spin at a frequency around 10^{-3} Hz. The three-axis 120 kg MICROSCOPE satellite will be launched in 2007 by a Dnepr rocket (to be confirmed) into a Sun-synchronous, quasicircular (eccentricity 10^{-2}) orbit at 700 km altitude. The drag from the residual atmosphere and solar radiation pressure will be compensated for by a system of proportional FEEP thrusters. A total of 8–12 thrusters, each with a thrust authority of 150 μN, will be employed. Their noise level must not exceed $0.1\,\mu\mathrm{N\,Hz^{-1/2}}$ to provide the required drag-free control performance of $3 \cdot 10^{-10}\,\mathrm{m\,s^{-2}\,Hz^{-1/2}}$ in the measurement bandwidth [16]. The FEEP thrusters also serve as actuators for fine attitude control.

4.6 Further Applications

In the missions described in the sections before, the drag-free control system is closely connected to the experiment. In most of the missions the test masses for the drag-free control system are the central part of the experiment. Besides this configuration a more decoupled application can be imagined.

First, the drag-free control system can be used to generate a high-quality microgravity environment for experiments. These experiments are not connected to the drag-free control system. The DFC simply serves as a very accurate control system of the spacecraft bus. Thus the capabilities of a satellite are extended by adding the drag-free control system.

Secondly, the drag-free control system can be used to decouple very sensitive subsystems from external disturbances. If we consider a highly sensitive experiment in a box as the test mass, it can be shielded by the surrounding satellite. Then the experiment box is free from all external disturbances.

This concept was already studied for the Hubble Space Telescope successor the James Webb Space Telescope (or Next Generation Space Telescope – NGST; see [9, 10]). This concept offers the opportunity for high-accuracy pointing even in orbits with large disturbances.

5 Summary

The drag-free control technology has become an enabling technology for current and future space missions in the area of fundamental physics, geodesy, and also microgravity research. Although the idea of the drag-free controlled satellite is already 40 years old [8], it has taken the time to develop the needed sensor and actuator technologies for applying the idea of the drag-free satellite.

Today the drag-free technology is mainly used for fundamental physics but future space missions in other areas may utilize this technology and its variations.

References

1. E. Canuto, P. Martella, and G. Sechi. The GOCE Drag Free and Attitude Control Design Aspects and Expected Performance. In *Proceedings of the 5th International Conference on Spacecraft Guidance, Navigation and Control Systems; Frascati, Italy*, October 2002.
2. Giuseppe Catastini. The GOCE End-To-End System Simulator. In *2nd International GOCE User Workshop, ESA ESRIN*, March 2004.
3. Triad I. A Satellite Freed of all but Gravitational Forces. *Journal of Spacecraft*, 11(9), 1974.
4. Yusuf R. Jafry. *Aeronomy Coexperiments on Drag-Free Satellites with Proportional Thrusters: GP-B and STEP.* PhD thesis, Department of Aeronautics and Astronautics of Stanford University, March 1992.
5. M. Kersten and A. Schleicher. Integrated Modeling of the Laser Interferometer Space Antenna (LISA). In *Proceedings of the International Symposium on Formation Flying, Toulouse, France*, October 2002.
6. H. Klotz, H. Strauch, W. Wolfsberger, S. Marcuccio, and C. Speake. Drag-Free, Attitude and Orbit Control for LISA. In *Third International Conference on Spacecraft Guidance, Navigation and Control Systems; ESTEC, Noordwijk, Netherlands*, volume ESA SP-381. ESA, November 1996.
7. K. Kurmakaev. On the Gravitational Effects on the Motion of Extended Rigid Bodies. Master's thesis, Faculty of Applied Mathematics and Economics of the Moscow Institute of Physics and Technology, June 2003. In Russian.
8. Benjamin Lange. *The Control and Use of Drag-Free Satellites.* PhD thesis, Department of Aeronautics and Astronautics of Stanford University, June 1964.
9. N. Pedreiro. Disturbance-free Payload Concept Demonstration. In *AIAA/AAS Astrodynamics Specialist Conference, Monterey, California*, August 2002.
10. N. Pedreiro. Spacecraft Architecture for Disturbance-free Payload. In *AIAA/AAS Astrodynamics Specialist Conference, Monterey, California*, August 2002.
11. J. Courtney Ray. *Partially Drag-Free Satellites with Application to the TIP II Satellite.* PhD thesis, Department of Aeronautics and Astronautics of Stanford University, 1976.
12. X. Sembely, L.Vaillon, and O. Vandermarq. High Accuracy Drag-Free Control for The Microscope and The Lisa Missions. In *Proceedings of the 5th International Conference on Spacecraft Guidance, Navigation and Control Systems; Frascati, Italy*, October 2002.

13. STEP. Phase A Interim Report. Technical report, NASA/ESA Joint STEP Working Group, 2001.
14. Stephan Theil. *Satellite and Test Mass Dynamics Modeling and Observation for Drag-free Satellite Control of the STEP Mission*. PhD thesis, Department of Production Engineering, University of Bremen, December 2002.
15. L. Vaillon and C. Champetier. Drag-Free & Attitude Control System for the Gravity Explorer Mission. In *Third International Conference on Spacecraft Guidance, Navigation and Control Systems; ESTEC, Noordwijk, Netherlands*, volume ESA SP-381. ESA, November 1996.
16. A. Wilson, editor. *ESA's report to the 34th COSPAR meeting*, volume 1259 of *ESA SP*. European Space Agency, Nordwijk, 2002.